Research Article
Evaluation of Residual Stresses Induced by Face Milling Using a Method of Micro-indents

[1]F.V. Díaz, [1]C.A. Mammana and [2]A.P.M. Guidobono
[1]Departamento de Ingeniería Electromecánica-Departamento de Ingeniería Industrial, Facultad Regional
Rafaela, Universidad Tecnológica Nacional, Acuña 49, 2300 Rafaela, Argentina
[2]División Metrología Dimensional, Centro Regional Rosario (INTI), Ocampo y Esmeralda,
2000 Rosario, Argentina

Abstract: The aim of this study is to determine and evaluate residual stresses induced by face milling in different zones, which are associated with asymmetries in orientation of cutting edge. In this study, a micro-indent method is used to determine these stresses, which were induced in samples of AA 7075-T6 aluminum alloy. The residual displacements were measured, with high accuracy, using a universal measuring machine. This study includes a thorough data analysis using Mohr's circles, which enabled to assess the stress states in all in-plane directions. The results obtained in samples subjected to different combinations of process parameters showed the introduction of compressive normal components for all directions of each zone evaluated. From the high sensitivity of the micro-indent method used, it was possible to detect smaller differences generated between the levels reaching the stress components in the cutting zones evaluated. Furthermore, these differences were similar for all evaluated directions when the highest feed rate was selected. This significant fact, finally, would reveal equivalent differences between asymmetrical zones, regarding the combination of local plastic deformation and heat reaching the milled surface, for all in-plane directions.

Keywords: Aluminum alloy, face milling, micro-indentation, Mohr's circle, residual stresses

INTRODUCTION

Residual stresses developed in components of machines and structures often lead to catastrophic failures (Rowlands, 1987). This kind of stress can be defined as the ones existing in a solid, even in the absence of forces and/or moments. The introduction of these stresses is very common during the different kind of material processing such as welding, rolling or machining. In many cases, tensile residual stresses are associated with early failures generated by fatigue, corrosion or wear (Toribio, 1998; Schwach and Guo, 2006). In contrast, compressive stresses are typically induced in order to strengthen mechanical components under the same load conditions (Van Boven *et al.*, 2007; Benedetti *et al.*, 2010).

In a mechanical component, residual stresses are developed when it undergoes non uniform plastic deformation and/or it is subjected to thermal gradients. When a new surface is generated by machining, a large local plastic deformation occurs and also a large amount of heat is transferred to a surface layer of very narrow thickness (Trent, 1991). Thus, the origin of residual stresses introduced by machining is both mechanical and thermal. The local plastic deformation degree and the amount of heat in surface layer will depend, for a given material, on the process parameters selected, on the geometry, design and state of cutting tool and also on cooling conditions (Brinksmeier *et al.*, 1982).

Face milling is very common in the industry. In this kind of milling, the instantaneous orientation of cutting-edge changes in relation to an orthogonal reference system fixed on the milled surface (Jacobus *et al.*, 2001). This change implies that the chip formation process and the associated plastic deformation will instantly change in orientation, which will influence the residual stress introduction. In addition, the chip thickness will adjust continuously, generating instantaneous changes regarding heat flow from the primary deformation zone to the surface generated (Trent, 1991). Thus, the temperature of the new surface will constantly change due to cutting-edge movement, affecting the residual stress introduction.

The purpose of this study is to evaluate and compare residual stresses, introduced by face milling,

Fig. 1: Upper view of the tool-sample system

Fig. 2: State of residual stress at a point of the milled surface
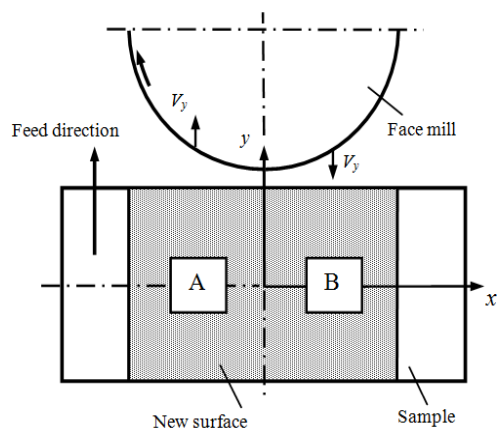
in two zones, which were generated from asymmetries in the orientation of cutting edge. It is noteworthy that, in most relevant published studies (Henriksen, 1951; Okushima and Kakino, 1971; Okushima and Kakino, 1972; Matsumoto *et al*., 1986; Wu and Matsumoto, 1990; M`Saoubi *et al*., 1999; Capello, 2005; Rao and Shin, 2001), the analysis does not take into account the changes occurring in the residual stress due to the path of cutting edge on different zones, which play an important role in both geometric distortion and service life. In this study, the normal and tangential components of residual stress were determined using a micro-indent method (Wyatt and Berry, 2006). Face milling tests were conducted on samples of AA 7075-T6 aluminum alloy using a numerically controlled machining centre. The feed rate was varied to assess the effects generated in the tangential and normal components of residual stress. The evaluation of these effects allowed us to detect that the plastic stretching difference between both evaluated zones is independent of the feed rate for some preferential in-plane directions. Finally, this fact implies that, for these directions, the combination of the amount of local plastic deformation (mechanical effect) and the heat reaching the milled surface (thermal effect) will present equivalent differences between the centroids of both cutting zones evaluated.

MATERIALS AND METHODS

This study was carried out in the year 2016 at the Departamento Ingeniería Electromecánica, Facultad Regional Rafaela, Universidad Tecnológica Nacional of Argentina.

As previously mentioned, a thorough evaluation of different components of residual stress generated through face milling operations was carried out in this study. Figure 1 shows the new surface (63×40 mm) and the location of the points evaluated (A and B), which are in the centroids of the conventional ($x>0$, y) and climb ($x<0$, y) cutting zones (Trent, 1991). The samples
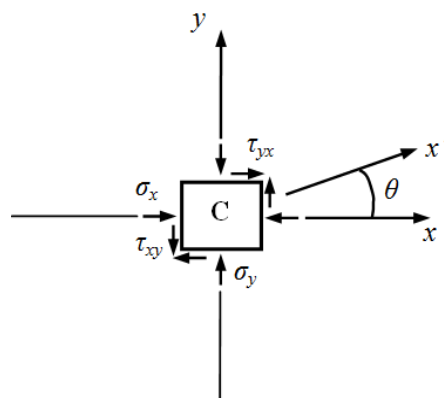
were milled in a numerically controlled vertical machining center (Victor Vc-55) installed in a laboratory. A balanced face mill of 63 mm in diameter was used. This face mill includes five inserts (Palbit SEHT 1204 AFFN-AL SM10) of tungsten carbide. The cutting speed and depth of cut were set at $V = 100$ m/min and $d = 0.4$ mm, respectively. Furthermore, the feed rate was varied from $f = 0.08$ mm/tooth to $f = 0.16$ mm/tooth in order to evaluate the residual stress variation in both cutting zones to be assessed. It should be noted that the feed per tooth is the linear displacement of the sample when the face mill rotates 1/5 of revolution.

The samples were prepared from a 4 mm thick rolled product of AA 7075-T6 aluminum alloy. Optical microscopy revealed a grain structure elongated along the rolling direction (TG: 40×8 μm) of solid solution α (Al) with precipitated particles (aligned in the rolling direction) of (Fe, Mn) Al_6 and $CuMgAl_2$. The micro-hardness of this product, evaluated from different points, averaged 186 HV0.5.

It is noteworthy that the face milling operations were conducted on residual stress free samples. The heat treatment to release these stresses was performed after preparing the geometry of the samples (110×40×4 mm). The parameters were 300°C and 80 min. Finally, the cooling process was carried out in the furnace (Dalvo HM2).

The details of the indent method implemented in this study can be consulted in previous studies (Díaz *et al*., 2010; Díaz and Mammana, 2012). Briefly, this technique consists, first, in introducing a micro-indent distribution at the surface evaluated. Secondly, the coordinates of the micro-indents are measured, before and after a thermal distension treatment, using a universal measuring machine. It should be noted that these machines enable performing high-accuracy measurements, including the determination of orthogonal coordinates (x, y, z) at different points of mechanical components through the inclusion of a high-precision microscope (Curtis and Farago, 2007).

Figure 2 shows the state of residual stress at any point of a surface generated by face milling (point C).

For obtaining the different components of stress at that point, four micro-indents must be introduced. These micro-indents are located in the corners of an imaginary square whose centroid is the point to evaluate (Mammana *et al.*, 2010). In this study, the micro-indents were introduced using a micro-hardness tester Shimadzu HMV-2. As previously mentioned, the micro-indent coordinates were measured, before and after a thermal distension treatment (300°C during 80 min), using a universal measuring machine (GSIP MU-314). Then, by processing these coordinates (Díaz *et al.*, 2012), it is possible to obtain the components of residual strain ε_x, ε_y and γ_{xy}, which correspond to the centroid of the square mentioned. Assuming that each milled surface is evaluated under conditions of plane stress and considering that the material is homogeneous, isotropic and linear elastic, the normal and tangential components of residual stress can be expressed as (Gere, 2001)

$$\sigma_{x'} = \frac{\sigma_x + \sigma_y}{2} + \frac{\sigma_x - \sigma_y}{2}\cos 2\theta + \tau_{xy} \cdot \sin 2\theta$$

$$\tau_{x'y'} = -\frac{\sigma_x - \sigma_y}{2}\sin 2\theta + \tau_{xy} \cdot \cos 2\theta \qquad (1)$$

where, σ_x, σ_y and τ_{xy}, obtained from ε_x, ε_y and γ_{xy}, are the components of residual stress associated to the original reference system (axes *x* and *y*) and θ is the angle between the direction *x′* and the reference axis *x* (Fig. 2).

The error associated with the procedure for residual stress determination was estimated to be ±0.9 MPa (Díaz *et al.*, 2010). The coordinates of micro-indents were measured, in a laboratory, within a temperature range of 20±0.2°C, with a variation less than 0.01°C/min. It is important to note that if this variation is greater than the mentioned value, the measurement error will significantly increase.

RESULTS AND DISCUSSION

Figure 3 shows the normal components σ_x and σ_y, which are predominantly compressive. This occurs because, in face milling, the secondary cutting-edge interacts intermittently with the sample, generating an elevated tensile strain behind the mentioned edge (Brinksmeier *et al.*, 1982). Then, the deformation zone is relaxed, leading to a state of compressive residual stress.

Figure 3a shows the component σ_x. It is important to note that the *x* direction is normal to feed direction. This figure shows that the maximum compressive values correspond to the centroid of the conventional cutting zone (point B). Moreover, the change in feed rate generates, in that point, a small negative increase. In contrast, in the centroid of the climb cutting zone (point A), the increase in feed rate generates a compressive decrease. Figure 3b shows the component
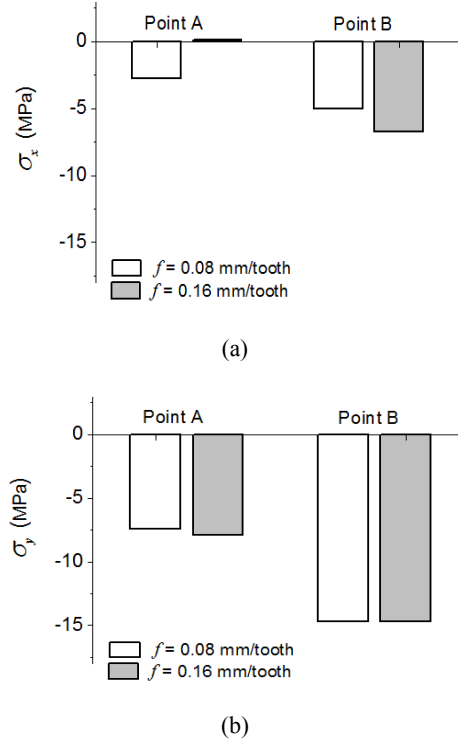

Fig. 3: Components (a) σ_x and (b) σ_y of the residual stress (cutting speed: $V = 100$ m/min, depth of cut: $d = 0.4$ mm)

σ_y. In a similar way to σ_x, the values associated with the point B are more negative than the ones in the point A. Furthermore, the increase in feed rate generates a more compressive state in A, while in B, the compressive level is maintained. The differences between the stress value corresponding to σ_y and σ_x would be due to the force of feed, which acts in the *y* direction. It is noteworthy that the small level differences between climb and conventional cutting are a result of the influence of the relative orientation between the V_y component and feed rate (Fig. 1) on the introduction of local plastic deformation (Díaz *et al.*, 2010).

The components σ_p and σ_q, which correspond to the principal directions, are shown in Fig. 4. It is important to note that, in these directions, the normal component $\sigma_{x'}$ reaches its maximum and minimum values (Gere, 2001). Figure 4a shows the component σ_q, which is, the smaller compressive principal component. The behavior of this component is similar to σ_x. Furthermore, Fig. 4b shows the more compressive principal component σ_p, which is analogous to σ_y. Both similarities reveal that the principal directions, which are perpendicular, would be very close to the reference orthogonal axes (*x* and *y*).

Different Mohr's circles were analyzed in order to assess the directions associated with the more compressive principal stress and also to understand the several states of residual stress generated by face milling. These circles are shown in Fig. 5. It is noteworthy that the orthogonal coordinates at each point of each circle represent the values of the residual
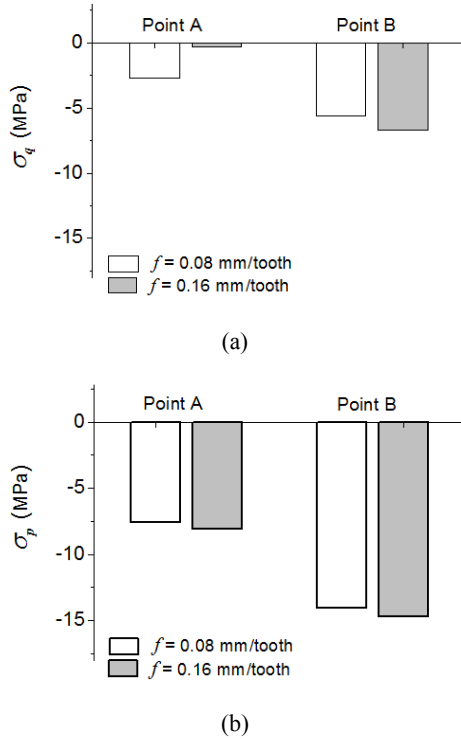
Fig. 4: Components (a) σ_q and (b) σ_p of the residual stress (cutting speed: $V = 100$ m/min, depth of cut: $d = 0.4$ mm)

stress components corresponding to a system reference rotated an angle θ. In addition, the segment intersecting each circle indicates the reference direction ($\theta = 0$ in Fig. 2).

The circles corresponding to $f = 0.08$ mm/tooth are shown in Fig. 5a. As expected, the more compressive circle corresponds to the point B (conventional cutting zone), where the directions of V_y and feed rate are opposite (Fig. 1). An important feature of this figure is that the circles overlap. This would indicate that, for those overlapped directions, the cutting conditions, corresponding to conventional milling, would generate similar plastic modifications in both zones evaluated. Another peculiarity is that the relationship between the diameters of the circles associated with B and A is approximately 2. This fact implies that both the maximum shear stresses and the anisotropy degree of the normal components in B doubled those in A. Furthermore, both circles show very similar reference directions ($\theta = 0$), which would indicate that for the combination of milling parameters evaluated, the path of cutting tool does not generate directional changes and therefore, the principal directions would be equivalent for both centroids.

The circles corresponding to $f = 0.16$ mm/tooth are shown in Fig. 5b. In this case, the stress anisotropy is equivalent in both centroids because the diameters are similar. This fact reveals that the introduction of shear residual stresses is independent of the zone evaluated. In addition, the angular range containing the reference directions corresponding to $\theta = 0$ is very low (8.6°). Furthermore, when the homologous circles of Fig. 5a and b are compared it is possible to note that the increase in feed rate modifies the diameters of circles, but not the relative position (the more compressive circles correspond to the centroid B). The diameter change implies that the stress anisotropy increases in A
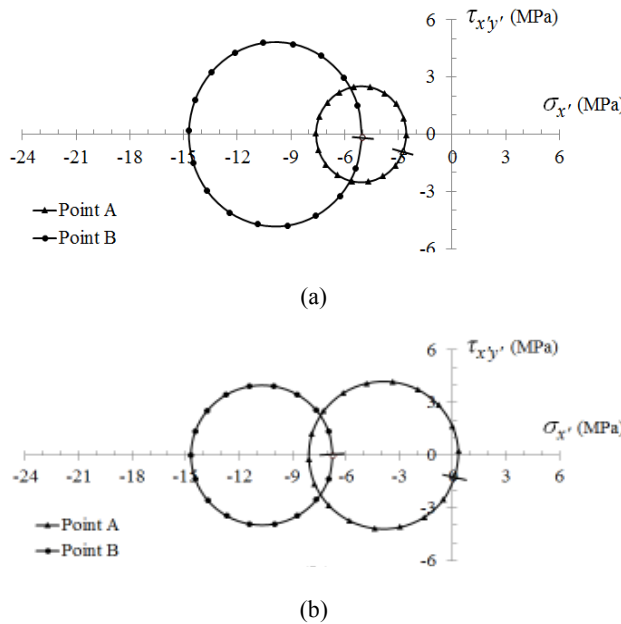

Fig. 5: Mohr's circles corresponding to the points A and B (cutting speed: $V = 100$ m/min, depth of cut: $d = 0.4$ mm, feed rate: (a) $f = 0.08$ mm/tooth and (b) $f = 0.16$ mm/tooth)
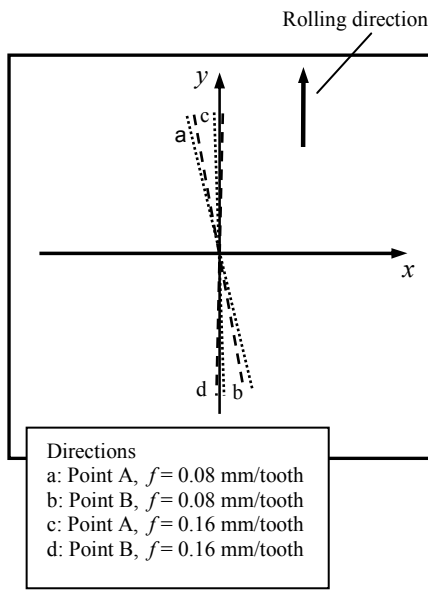
Fig. 6: Directions corresponding to the more compressive principal component

Table 1: Normal component variation between centroids

Component	f = 0.08 mm/tooth	f = 0.16 mm/tooth
σ_x	2.26	6.87
σ_y	7.27	6.80
σ_q	2.89	6.40
σ_p	6.47	6.67
σ_m	4.68	6.51

$\Delta\sigma$ (MPa)

and decreases in B. In addition, it is possible to observe that, for homologous circles, the reference directions (θ = 0) are similar, which would reveal that the directions of principal and maximum shear components of residual stress would be independent, for each centroid, of the feed rate selected.

Figure 6 shows the directions associated with the more compressive principal component. In all cases, this component is very close to the axis y, which corresponds to the feed rate direction and also to the rolling direction of the material evaluated. It is noteworthy that the angular range covered by this component is very low (10.7°). These results corroborate the ones obtained by comparing the behavior of two aluminum alloys subjected to high speed milling conditions (Díaz *et al*., 2012). From both studies, it is possible to infer the important role played by the rolling direction regarding the different states of residual stress obtained.

In addition, Table 1 shows the variation of different normal components between the centroids A and B. It is noteworthy that the component σ_m corresponds to the average value of the principal components. All variations showing Table 1 are positive, which means that the values in B are, for all cases, more compressive than in A. The most outstanding feature of this table is that, for the σ_p and σ_y components, the increments are independent of feed rate because the differences are not significant. Díaz *et al*. (2015) showed a similar behavior for the σ_m component when tests corresponding to medium and high speed milling were carried out. On the other hand, the highest stress increments were obtained for f = 0.16 mm/tooth. This fact implies that, for the cutting conditions including this feed rate, greater differences in the plastic

stretching between both centroids are generated. This could be due to a larger difference in the adaptation of the cutting edge in both zones when f = 0.16 mm/tooth is selected.

Table 1 shows that, for feed rate of 0.16 mm/tooth, the change of different components of residual stress is independent of the direction evaluated. Therefore, the plastic stretching difference between both centroids will be equivalent to the in-plane directions associated with the most significant normal components. This implies that the combination of the local plastic strain amount (mechanical effect) and the heat reaching the milled surface (thermal effect) will show similar differences between both centroids. It is important to note that these differences occur in directions associated with principal and maximum shear stresses and also in directions corresponding to the original reference system. Finally, because the Mohr's circles in Fig. 5b show equivalent diameters and reference directions, it is possible to infer that the aforementioned differences in the combination of mechanical and thermal effects are present in all in-plane directions.

CONCLUSION

The micro-indent method used in this study allowed to determinate, with very high accuracy, normal and tangential components of residual stress, which were generated by face milling in samples of AA 7075-T6 aluminum alloy. These components were determined in the climb and conventional cutting zones, which show asymmetries due to changes in orientation of cutting edge. The feed rate, which is a main process parameter, was varied to assess the effects generated in the mentioned zones. The normal components were always more compressive in the conventional cutting zone because, in this zone, the V_y component of cutting speed and the feed rate have opposite directions. Moreover, when face milling is performed at the greatest feed rate, both the increments of residual stress and the difference in plastic stretching between the milled zones will be the highest. This fact may be associated with additional difficulties in the adaptation of cutting edge in both zones evaluated. Furthermore, the residual stress states associated with the highest feed rate showed the same degree of anisotropy and similar orientation in the principal directions of the two zones. Finally, the increases of stress were, for the mentioned feed rate, independent of the direction evaluated, which implies that the combination of local plastic strain amount (mechanical effect) and the heat

reaching the milled surface (thermal effect) presents, for all in-plane directions, equivalent differences between the centroids evaluated.

ACKNOWLEDGMENT

REFERENCES

Benedetti, M., V. Fontanari and B.D. Monelli, 2010. Plain fatigue resistance of shot peened high strength aluminium alloys: Effect of loading ratio. Proc. Eng., 2(1): 397-406.

Brinksmeier, E., J.T. Cammett, W. König, P. Leskovar, J. Peters and H.K. Tönshoff, 1982. Residual stresses-measurement and causes in machining processes. CIRP Ann-Manuf. Techn., 31(2): 491-510.

Capello, E., 2005. Residual stresses in turning: Part I: Influence of process parameters. J. Mater. Process. Tech., 160(2): 221-228.

Curtis, M.A. and F.T. Farago, 2007. Handbook of Dimensional Measurement. Industrial Press Inc., New York.

Díaz, F.V., R.E. Bolmaro, A.P.M. Guidobono and E.F. Girini, 2010. Determination of residual stresses in high speed milled aluminium alloys using a method of indent pairs. Exp. Mech., 50(2): 205-215.

Díaz, F.V. and C.A. Mammana, 2012. Study of residual stresses in conventional and high-speed milling. In: Filipovic, L.A. (Ed.), Milling: Operations, Applications and Industrial Effects. Nova Science Publishers, Inc., New York, pp: 127-155.

Díaz, F., C. Mammana and A. Guidobono, 2012. Evaluation of residual stresses induced by high speed milling using an indentation method. Modern Mech. Eng., 2(4): 143-150.

Díaz, F.V., C.A. Mammana and A.P.M. Guidobono, 2015. Evaluation of residual stresses in low, medium and high speed milling. Res. J. Appl. Sci. Eng. Technol., 11(3): 252-258.

Gere, J.M., 2001. Mechanics of Materials. 5th Edn., Brooks/Cole, Pacific Grove, CA.

Henriksen, E.K., 1951. Residual stress in machined surfaces. Trans. ASME, 73: 69-76.

Jacobus, K., S.G. Kapoor and R.E. DeVor, 2001. Experimentation on the residual stresses generated by endmilling. J. Manuf. Sci. Eng., 123(4): 748-753.

Mammana, C.A., F.V. Díaz, A.P.M. Guidobono and R.E. Bolmaro, 2010. Study of residual stress tensors in high-speed milled specimens of aluminium alloys using a method of indent pairs. Res. J. Appl. Sci. Eng. Technol., 2(8): 749-756.

Matsumoto, Y., M.M. Barash and C.R. Liu, 1986. Effect of hardness on the surface integrity of AISI 4340 steel. J. Eng. Ind., 108(3): 169-175.

M`Saoubi, R., J. Outeiro, J. Changeux, J.L. Lebrun and A. Morão Dias, 1999. Residual stress analysis in orthogonal machining of standard and resulfurized AISI 316L steels. J. Mater. Process. Tech., 96(1-3): 225-233.

Okushima, K. and Y. Kakino, 1971. Residual stress produced by metal cutting. Ann. CIRP, 20: 13-14.

Okushima, K. and Y. Kakino, 1972. A study on the residual stress produced by metal cutting. Memoirs of the Faculty of Engineering, Kyoto University, 34: 234-248.

Rao, B. and Y.C. Shin, 2001. Analysis on high-speed face-milling of 7075-T6 aluminum using carbide and diamond cutters. Int. J. Mach Tool. Manu., 41(12): 1763-1781.

Rowlands, R.E., 1987. Residual Stresses. In: Kobayashi, A. (Ed.), Handbook on Experimental Mechanics. Prentice-Hall, New Jersey, pp: 768-813.

Schwach, D.W. and Y. Guo, 2006. A fundamental study on the impact of surface integrity by hard turning on rolling contact fatigue. Int. J. Fatigue, 28(12): 1838-1844.

Toribio, J., 1998. Residual stress effects in stress-corrosion cracking. J. Mater. Eng. Perform., 7(2): 173-182.

Trent, E.M., 1991. Metal Cutting. Butterworth and Heinemann, London.

Van Boven, G., W. Chen and R. Rogge, 2007. The role of residual stress in neutral pH stress corrosion cracking of pipeline steels. Part I: Pitting and cracking occurrence. Acta Mater., 55(1): 29-42.

Wu, D.W. and Y. Matsumoto, 1990. The effect of hardness on residual stresses in orthogonal machining of AISI 4340 steel. J. Eng. Ind., 112(3): 245-252.

Wyatt, J.E. and J. Berry, 2006. A new technique for the determination of superficial residual stresses associated with machining and other manufacturing processes. J. Mater. Process. Tech., 171(1): 132-140.